JOURNAL OF APPLIED ELECTROCHEMISTRY **10** (1980) 749–755

Anodization of lead in sulphuric acid solutions containing antimony species

F. ARIFUKU, H. YONEYAMA, H. TAMURA

Department of Applied Chemistry, Faculty of Engineering, Osaka University, Suita, Osaka, Japan

Received 23 December 1979

The influence of antimony in solution on the oxidation behaviour of lead in 5 M H_2SO_4 was studied by measuring the current–time curves during potentiostatic oxidation at 1.5 and 1.6 V, and by analysing the incorporated antimony in the resulting oxide layer as a function of depth. Antimony (III) species greatly influence the oxidation behaviour, but not so antimony (V). The amount of antimony incorporated was found to increase with the oxidation time in the electrolyte containing antimony (III), but in the antimony (V) solution it was almost constant at a relatively low level. The antimony incorporated from the antimony (III) solution was eluted by reoxidizing the oxide layer in an antimony-free solution, and the elution process was found to be accompanied by rearrangement of the oxide layer structure. The incorporation of antimony from the antimony (III) solution seems to be related to a complicated oxide formation process.

1. Introduction

Performance characteristics of lead–acid batteries are influenced by the presence of antimony in the positive grid [1–3] as well as in the paste [4], and many efforts have been made to elucidate the role of antimony [5–17]. It is well known that antimony in the grid dissolves into the electrolyte during the charge–discharge cycles and some of the dissolved antimony is adsorbed or incorporated again into the positive plate and possibly causes a change in the performance characteristics of the positive plates. The behaviour of antimony species in the electrolyte was reported by Dawson *et al.* [18], and the significant effects of antimony (III) species were also reported [19]. However, detailed information on antimony species in the electrolyte and the positive plate remains ambiguous.

As a step in the study of this problem, the effects of antimony species in the electrolyte on the oxidation behaviour of lead were investigated mainly by measuring the current–time response obtained during the potentiostatic oxidation of lead. The information derived from this source was combined with analysis of the oxide layer, to clarify the role of antimony in the oxidation behaviour of lead.

2. Experimental

2.1. *Preparation of samples*

Circular lead plates (99.999%, 16 mm diameter, 2 mm thick) were used as the test electrodes. These were polished mechanically and then electrochemically before mounting in a Teflon electrode holder, as reported previously [16]. The electrode was pre-cathodized at − 1.2 V for 30 min in 5 M H_2SO_4 to ensure a reproducible surface, and the electrolyte was then changed to the test solution. The electrode was then polarized to the desired anodic potentials where PbO_2 is predominantly formed.

5 M H_2SO_4 was prepared from reagent grade sulphuric acid and doubly distilled water, and prepurified by electrolysis. Electrolytes containing antimony (III) species were prepared by dissolving an Sb_2O_3 powder in 5 M H_2SO_4. Electrolytes containing antimony (V) species were prepared by adding hydrogen peroxide to the antimony (III) solution and then by boiling in the presence of platinum metal to destroy excess peroxide [18]. An $Hg/Hg_2SO_4/5$ M H_2SO_4 reference electrode was used. All the experiments were carried out at 25° C.

0021–891X/80/060749–07$02.70/0

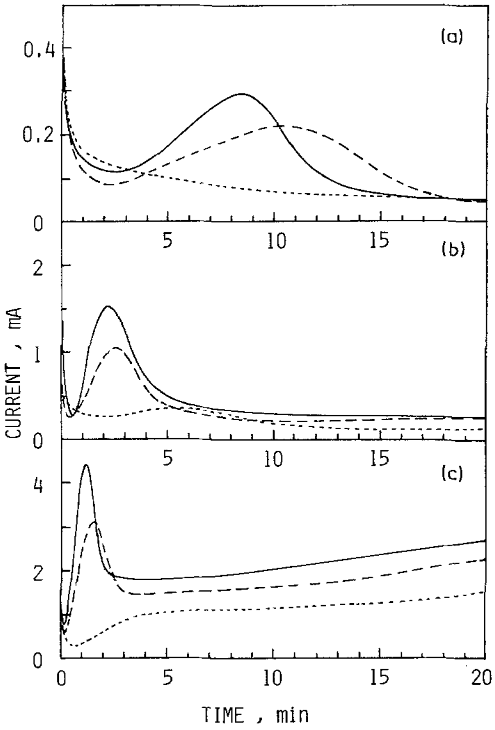

Fig. 1. Current–time curves for the potentiostatic oxidation of Pb in 5 M H_2SO_4 and 5 M H_2SO_4 containing either 2×10^{-3} M Sb (III) or 2×10^{-3} M Sb (V). (a) 1.40 V, (b) 1.50 V, (c) 1.60 V. —— 5M H_2SO_4, ------ 5 M H_2SO_4 containing 2×10^{-3} M Sb (III), – – – – 5 M H_2SO_4 containing 2×10^{-3} M Sb (V).

2.2. *Ion microprobe mass analysis*

Distribution profiles for antimony in the anodic films on lead, prepared under a variety of conditions, were analysed as a function of depth by using an ion microanalyser (Hitachi, model IMA-2). The diameter of the primary Ar^+ beam was 0.5 mm and the beam current was 0.5 μA. The other details of the analysing procedures have already been reported [16].

3. Results and discussion

The current–time curves obtained during the potentiostatic oxidation of Pb in 5 M H_2SO_4 and after the addition of either 2×10^{-3} M Sb(III) or 2×10^{-3} M Sb(V) are shown in Fig. 1. It is seen that the shape of the curve is similar in the electrolytes with and without antimony (V) irrespective of the polarization potentials. The minor differences are in the position of the current peaks, which appear as a result of lateral overlaps of lead dioxide crystals [20–22]; the peak heights were also somewhat depressed by the presence of antimony (V). Compared with antimony (V), antimony (III) had a remarkable influence. The current peak disappears completely at 1.40 V, and at 1.50 V only a small current peak with a large delay was observed. At 1.60 V the peak did not appear, and only an increase to a current plateau was observed.

Fig. 2 shows SEMs of the oxidized surfaces of Pb which were prepared by passing 1 C at 1.60 V in the three electrolytes used in Fig. 1. Large cubes observed in Fig. 2a and c are believed to be $PbSO_4$ which were produced during the washing of the sample with water; the corresponding crystals in the case of the antimony (III) solution (Fig. 2b) are spherulites. These differences may be

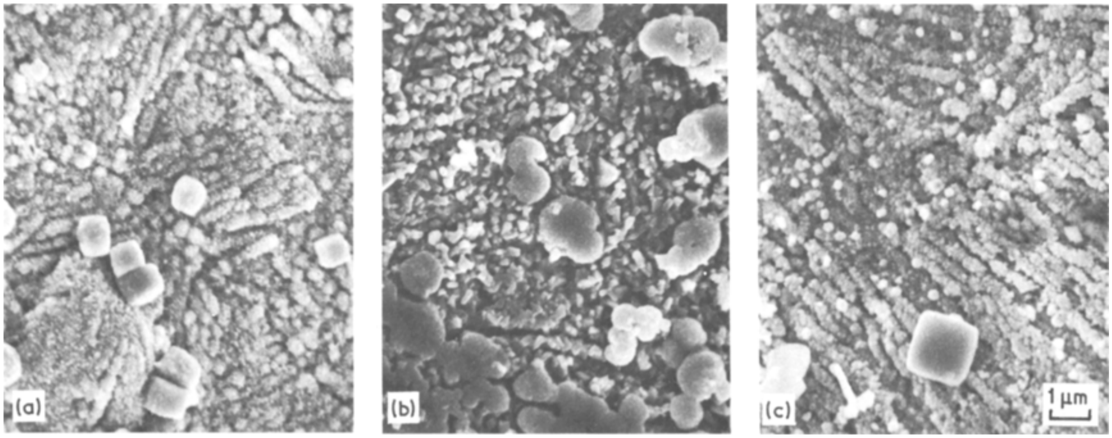

Fig. 2. SEMs of the surface of the oxide films formed by passing 1 C at 1.60 V in (a) 5 M H_2SO_4, (b) 5 M H_2SO_4 containing 2×10^{-3} M Sb (III), (c) 5 M H_2SO_4 containing 2×10^{-3} M Sb (V).

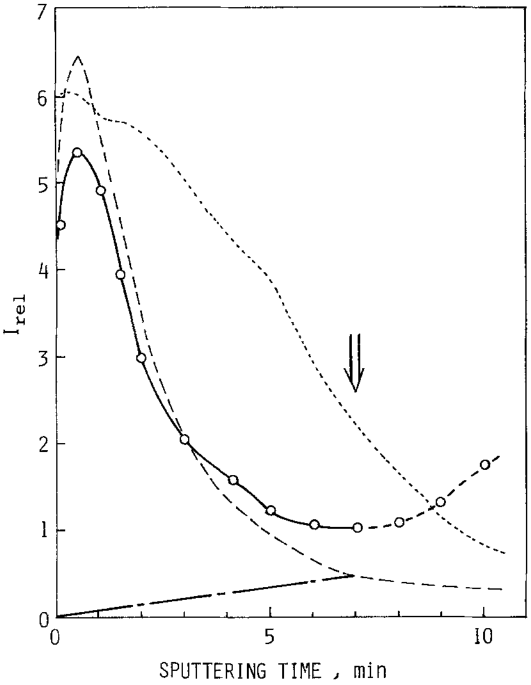

Fig. 3. Typical in-depth profiles of SbO_2^-, PbO_2^- and relative signal intensity ratio, $I_{SbO_2^-}/I_{PbO_2^-}$ (I_{rel}), for an oxide layer formed by passing 3 C at 1.50 V in 5 M H_2SO_4 containing 2×10^{-3} M Sb (III). The arrow indicates the oxide–substrate interface. ------ PbO_2^- (× 5); — — — — — SbO_2^- (× 1); – – – correction.

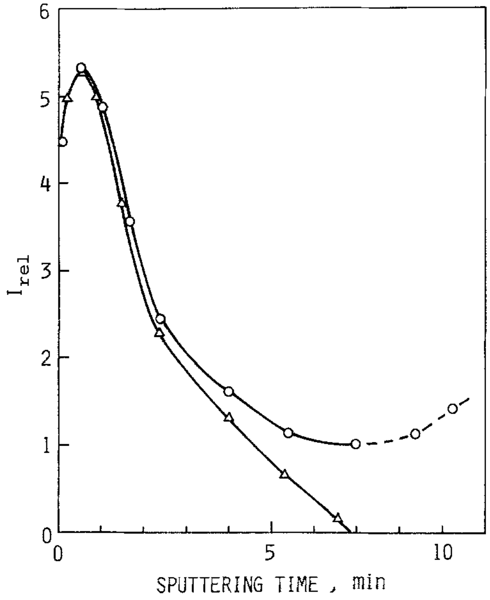

Fig. 4. Comparison of corrected I_{rel} with uncorrected values. ○: uncorrected, △: corrected.

related to the observation that the rate of self-discharge was greatly enhanced in the antimony (III) electrolyte [19]. Furthermore, the particle morphology of PbO_2 crystals formed in both antimony-free and antimony (V) solutions showed columnar arrays made up of very fine crystals, while the oxide formed in the antimony (III) solution was composed of definite crystallites with irregular distribution. These results show clearly that antimony (III) in solution has a great influence on the morphology of the resulting oxides, but not so antimony (V). The difference observed will be a reflection of the difference of the composition of the resulting oxides, which is described below.

Fig. 3 shows secondary ion signals of PbO_2^- and SbO_2^-, and the relative intensity ratio of these signals, $I_{SbO_2^-}/I_{PbO_2^-}$ (I_{rel}), for the oxide film formed by passing 3 C in the antimony (III) solution at 1.50 V. The position of the oxide–substrate interface is judged to be that shown with an arrow in the figure, because I_{rel} shows a minimum in this place. The SbO_2^- signal should not then be detected beyond this point, but was usually detected due possibly to inhomogeneity of and fluctuation in the impinging ion beam of the IMA. In order to give zero signal intensity of SbO_2^- at the point showing the minimum I_{rel}, an artificial correction was made in such a manner that the signal intensity of SbO_2^- to be subtracted is a linear function with depth reaching the observed intensity at the interface of the film and substrate. The I_{rel} profiles thus corrected are shown in Fig. 4 together with the uncorrected profile. As may be seen, there is no appreciable difference in the profiles of antimony in the region where the signal intensity is relatively high.

It has already been reported that the oxidation behaviour of lead to give lead dioxide is different at potentials positive and negative to 1.55 V [17, 23]. The incorporation of antimony species from the electrolytes was examined for oxide films prepared at 1.50 and 1.60 V.

Fig. 5 shows the profiles of antimony incorporated in the oxide films formed at 1.50 V in 5 M H_2SO_4 containing either 2×10^{-3} M Sb (III) or 2×10^{-3} M Sb(V). Similar results for the oxidation at 1.60 V are given in Fig. 6. The charge used for the oxidation was 1 and 3 C. These figures show that at both oxidation potentials, I_{rel} is high for the oxide films formed in the anti-

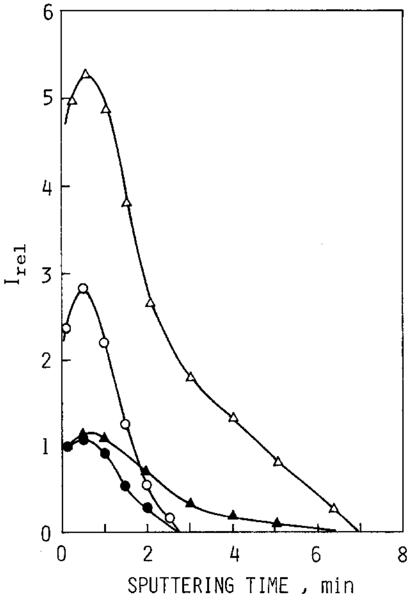

Fig. 5. Corrected I_{rel} profiles in the direction of oxide films formed in 5 M H_2SO_4 containing either 2 × 10^{-3} M Sb (III) (○, △), or 2 × 10^{-3} M Sb (V) (●, ▲). The oxidation was made by passing 1 C (○, ●) and 3 C (△, ▲) at 1.50 V.

mony (III) solution. Furthermore, it increases with the amount of charge passed in the oxidation process. On the basis of these findings, there is no doubt that the antimony (III) is the species incorporated in the oxide layers. The incorporation in this case is due to the formation of complex oxide, as described in a later section. Some incorporation is also indicated by the data of Figs. 5 and 6 for Sb(V), but this is believed to be due to adsorption effects, because I_{rel} was not enhanced with the oxidation charge. According to Dawson *et al.* [18], antimony (V) is present as a stable anionic species and its adsorbability is high.

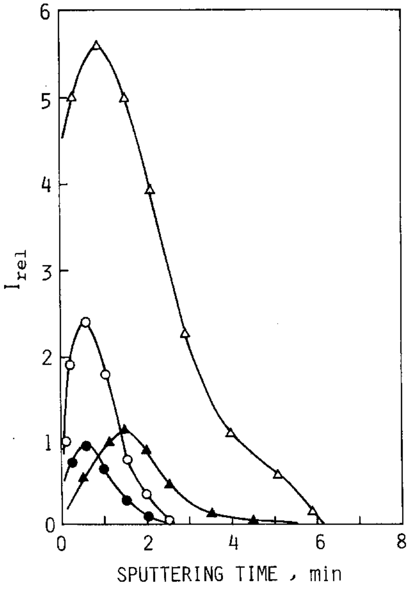

Fig. 6. As for Fig. 5, but at 1.60 V.

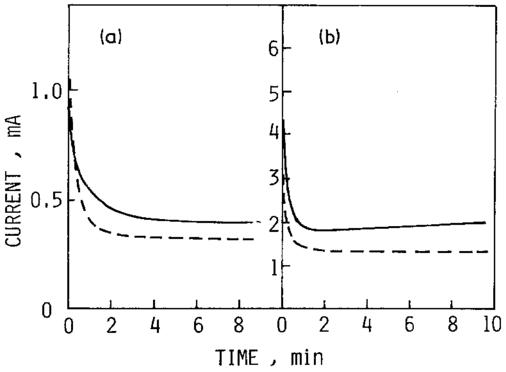

Fig. 7. Current–time curves during reoxidation in 5 M H_2SO_4 of the oxide layers formed by passing 1 C in 5 M H_2SO_4 (———) and the solution containing 2 × 10^{-3} M Sb (V) (– – – –). (a) 1.50 V; (b) 1.60 V.

The incorporation process of antimony (III) species and the stability of the incorporated antimony were investigated in detail. As already reported [17] and shown in Fig. 1, the current–time curves in the initial stage of potentiostatic oxidation of lead show characteristic features of a complex oxidation process. After completion of the current peak, the oxide growth proceeds to increase its thickness. Such situations were found to be realized when lead was anodically oxidized by passing 1 C at 1.50 V in 5 M H_2SO_4 whether or not 2 × 10^{-3} M Sb(V) was present, as judged from the results shown in Fig. 1. The same was true for the oxidation at 1.60 V. When the oxide samples prepared in this way were re-anodized in 5 M H_2SO_4, the current–time curves obtained showed a monotonic decrease to reach an almost steady value, as shown in Fig. 7. On the re-anodization in 5 M H_2SO_4 the oxide prepared in the antimony (V) solution showed a very similar behaviour to that prepared in the antimony-free solution. The close similarity indicates that antimony (V) has no significant influence on the nature of the lead dioxide formed. In contrast to these oxides, oxide samples prepared in the Sb(III) solution with passage of 1 C showed a quite different behaviour on the re-anodization in 5 M H_2SO_4. For example,

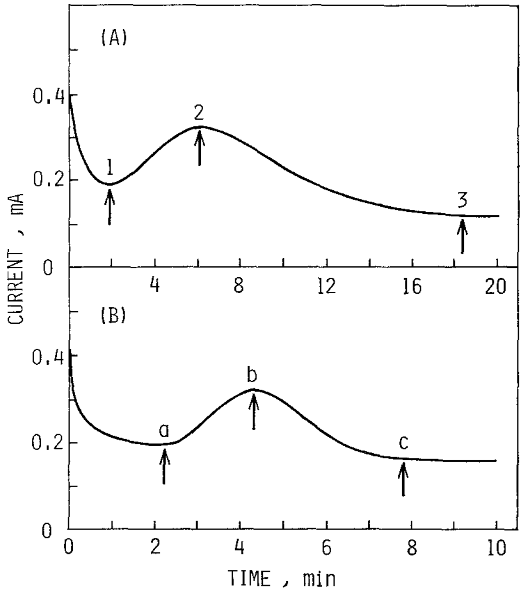

Fig. 8. Current–time curves for the potentiostatic oxidation of Pb in 5 M H_2SO_4 containing 2 × 10^{-3} M Sb (III) (A), followed by reoxidation in 5 M H_2SO_4 (B) at 1.50 V. The arrows indicate the oxidation steps for oxide film formation which are used in Figs. 10 to 12.

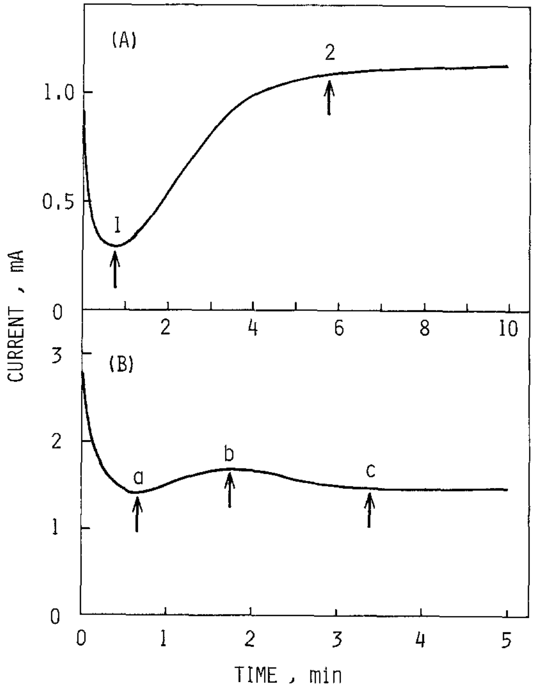

Fig. 9. As for Fig. 8, but at 1.60 V.

oxide samples prepared in 5 M H_2SO_4 containing 2 x 10^{-3} M Sb(III) at 1.50 V, where the current–time curve shown in Fig. 8A was obtained, were subjected to re-anodization in 5 M H_2SO_4, the current–time curves obtained showed a current peak as shown in Fig. 8B. Similar behaviour, though weak, was observed for the oxidation at 1.60 V, which is shown in Fig. 9. The appearance of the current peak on the anodization indicates that some change occurs in the crystal structure of the oxide layer, suggesting that the oxide formed in the antimony (III) solution is unstable.

Fig. 10 shows I_{rel} profiles for oxide layers prepared by passing current up to the time shown by arrows in Figs. 8A and 9A. The significance of the points shown by arrows has already been described [17]. It is known from the results in this figure that the signal profiles are strengthened with promotion of oxidation, as suggested from the results shown in Figs. 5 and 6. On the re-anodization of the oxide layer formed by passing 1 C, however, I_{rel} was found to noticeably decrease if the reoxidation is continued to stages beyond the oxidation step where the three-dimensional overlap of crystal centres is completed (point c, Figs. 8B and 9B). The results showing this are given in Figs. 11 and 12.

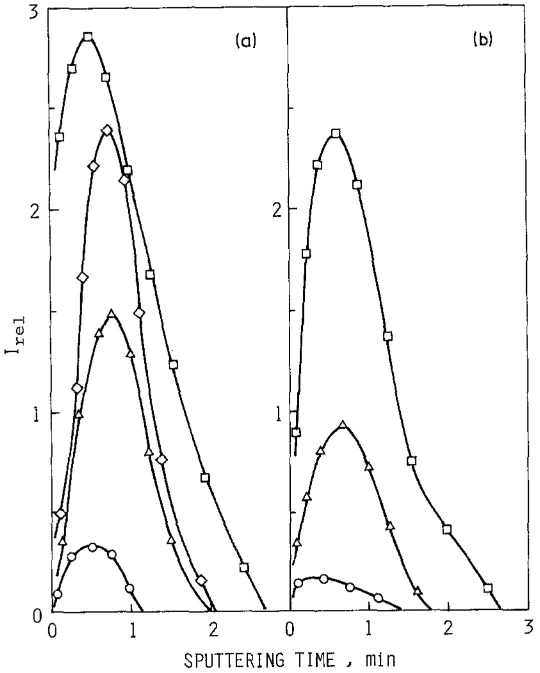

Fig. 10. Corrected I_{rel} profiles in the direction of oxide layer formed in 5 M H_2SO_4 containing 2 × 10^{-3} M Sb (III) at 1.50 V (a) and 1.60 V (b). The oxidation was continued to the time shown with numbered arrows in Figs. 8A and 9A. ○: 1, △: 2, ◇: 3, □: 1 C.

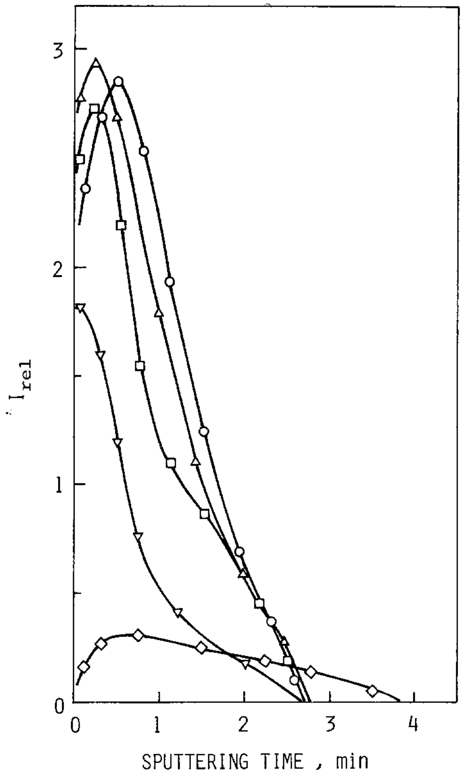

Fig. 11. Corrected I_{rel} profiles in the direction of oxide layers reoxidized in 5 M H_2SO_4 after the formation in 5 M H_2SO_4 containing 2 × 10^{-3} M Sb (III) by passing 1 C at 1.50 V. The reoxidation was made up to the time shown with alphabetized arrows in Figs. 8A and 9B. ○: 0 C, △: a, □: b, ▽: c, ◇: 1 C.

Since the area under the I_{rel} profiles (I_{rel} × time) reflects the amount of antimony in the oxide film, the area was plotted as a function of charge passed in the oxidation process. The results are given in Fig. 13. The open symbols in the figure are for the oxidation process in the antimony (III) solution, and the closed symbols are for the reoxidation process in the antimony-free solution. The results show that both the incorporation of antimony from the antimony (III) solution into the oxide film and the elution from the oxide film into the antimony-free solution are more prominent at 1.50 V than at 1.60 V.

The instability of the antimony incorporated into the oxide film from the antimony (III) solution seems to suggest that an unstable complexed oxide, which is composed of Pb^{2+}, Sb^{5+} and O^{2-} ions [24], is formed in the oxidation process. The potential chosen for the oxide formation is positive enough to give antimony (V), so that the incorporated antimony must have the pentavalent state. However, antimony (V) in solution seems not to be incorporated to give an oxide phase, as described above, and hence the incorporation of antimony

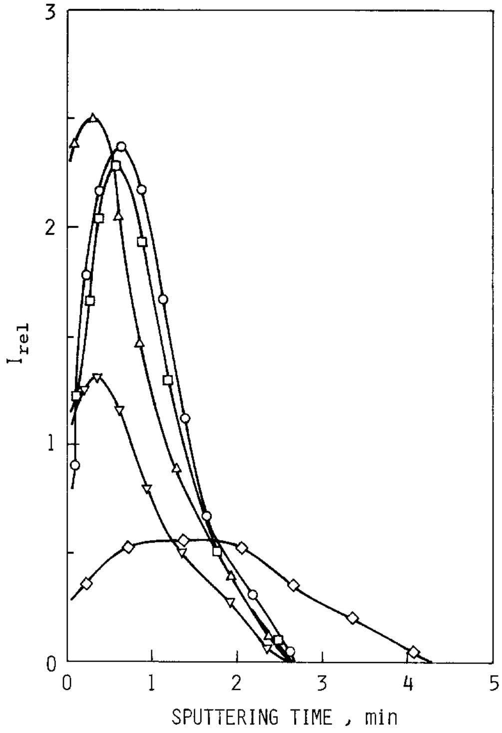

Fig. 12. As for Fig. 11, but at 1.60 V.

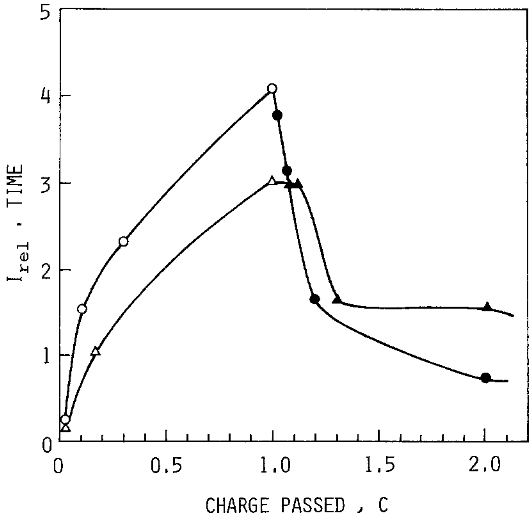

Fig. 13. Relationship between area of I_{rel} profiles and charge passed for oxidation. Open symbols: oxidation in 5 M H_2SO_4 containing 2 × 10^{-3} M Sb (III); closed symbols: reoxidation in 5 M H_2SO_4 subsequent to oxidation. ○, ●: 1.50 V, △, ▲: 1.60 V.

(III) must occur during the oxidation of lead. The fact that the incorporated antimony is stable in the antimony (III) solution but is lost on the reanodization in antimony-free solution seems to suggest that adsorption of antimony (III) stabilizes the complexed oxide in which not Pb (IV) but Pb (II) exists. Judging from the observations that a current peak during reoxidation periods appears to cause the loss of incorporated antimony, the loss is accompanied by the rearrangement of the three-dimensionally grown oxide. The rearrangement seems to be connected with the oxidation of Pb (II) to Pb (IV), leading to formation of lead dioxide. During the valence change of lead, the antimony is seemingly lost.

The results given in Fig. 13 show that the antimony content in the oxide layer was higher in the oxidation at 1.50 V than at 1.60 V. This seems to reflect the stability of Pb^{2+}. The more positive the electrode potential, the less stable is Pb (II).

These results are consistent with those obtained by potentiostatic oxidation of a Pb–Sb alloy in sulphuric acid solution, which was described in the previous paper [17].

References

[1] J. Burbank, *J. Electrochem. Soc.* **111** (1964) 1112.
[2] D. Kordes, *Chem. Ing. Tech.* 38 (1966) 638.
[3] E. J. Ritchie and J. Burbank, *J. Electrochem. Soc.* **117** (1970) 299.
[4] A. A. Abdul Azim and A. A. Ismail, *J. Appl. Electrochem.* 7 (1977) 119.
[5] J. Burbank and A. C. Simon, *J. Electrochem. Soc.* **110** (1953) 11.
[6] W. Herrmann and G. Pröpstl, *Z. Elektrochem.* **61** (1957) 1154.
[7] P. Rüetchi and B. D. Cahan, *J. Electrochem. Soc.* **105** (1958) 369.
[8] P. Rüetchi and R. T. Angstadt, *ibid* **105** (1958) 555.
[9] J. Burbank, *ibid* **111** (1964) 765.
[10] *Idem, ibid* **118** (1971) 525.
[11] M. P. J. Brennan, B. N. Stirrup and N. A. Hampson, *J. Appl. Electrochem.* 4 (1974) 49.
[12] T. F. Sharpe, *J. Electrochem. Soc.* **122** (1975) 845.
[13] J. L. Weininger and E. G. Siwek, *ibid* **123** (1976) 602.
[14] T. Rogatchev, S. T. Ruevski and D. Pavlov, *J. Appl. Electrochem.* 6 (1976) 33.
[15] T. F. Sharpe, *J. Electrochem. Soc.* **124** (1977) 168.
[16] F. Arifuku, H. Yoneyama and H. Tamura, *J. Appl. Electrochem.* 9 (1979) 629.
[17] *Idem, ibid* 9 (1979) 635.
[18] J. L. Dawson, J. Wilkinson and M. I. Gillibrand, *J. Inorg. Nucl. Chem.* **32** (1970) 501.
[19] J. L. Dawson, M. I. Gillibrand and J. Wilkinson, *Power Sources* 3 (1970) 1.
[20] M. Fleishmann and H. R. Thirsk, *Trans. Faraday Soc.* **51** (1955) 71.
[21] P. Casson, N. A. Hampson and K. Peters, *J. Electroanalyt. Chem.* 83 (1977) 87.
[22] E. M. L. Valeriote and L. D. Gallop, *J. Electrochem. Soc.* **124** (1977) 370.
[23] D. Pavlov and N. Iordanov, *ibid* **117** (1970) 1103.
[24] D. E. Swets, *ibid* **120** (1973) 925.